*J. Fluid Mech.* (1966), *vol.* 24, *part* 1, *pp.* 191–207
*Printed in Great Britain*



# The stability of a family of Jeffery–Hamel solutions for divergent channel flow

By P. M. EAGLES
Northampton College of Advanced Technology, London, E.C. 1

(Received 19 June 1965)

A set of Jeffery–Hamel profiles (for radial, viscous, incompressible flow) have been shown by Fraenkel (1962, 1963) to approximate to profiles in certain two-dimensional divergent channels. The stability of a family of these profiles is investigated by a numerical solution of the Orr–Sommerfeld problem. Neutral-stability curves are calculated in the $(R, k)$-planes (where $R$ is the Reynolds number of the basic flow and $k$ is the wave-number of the disturbance), and fairly low critical Reynolds numbers are found. For those profiles that have regions of reversed flow, negative wave velocities are found on the lower branch of the neutral curve, and also it is found that $Rk$ tends to a finite limit as $R \to \infty$ on the lower branch. These unexpected results are further discussed and verified by independent methods. The relation of the calculations to some experiments of Patterson (1934, 1935) is discussed.

## 1. Introduction

Fraenkel (1962, 1963) has shown that a certain set of Jeffery–Hamel (henceforth J.–H.) profiles, which are exact solutions for viscous, incompressible, steady, radial flow in a wedge-shaped channel, are good approximations to the profiles in certain symmetric, divergent channels with small wall-curvature. If $\alpha$, half the local divergence angle of the channel, varies smoothly and sufficiently slowly in a certain range containing $\alpha = 0$, then the approximate solution appropriate to the local $\alpha$ and a given Reynolds number† $R$ is uniquely determined from the infinite set of J.–H. solutions by the requirement that the stream function should be analytic as a function of $\alpha$. In this paper we consider the stability of a certain family of such flows, including some profiles with reversed flow near the walls.

In §2 the validity of the Orr–Sommerfeld equation is discussed for wedge-shaped channels and the problem selected for computation described. In §3 the method of computation is briefly described and its accuracy estimated. In §4 the main results are presented. Neutral stability curves in the $(R, k)$-planes (where $k$ is the wave-number of the disturbance) are given and very low values of the critical Reynolds number are found, in comparison with the critical values for parallel flow. More unexpectedly, the result was obtained that, on the lower

† For flow in a parallel-walled channel it is usual to use a Reynolds number based on the product of fluid velocity at the centre with channel half-width, but for a divergent channel it is better to use a Reynolds number $R$ based on half the volumetric flow rate, since this will not vary from station to station down the channel; and we therefore use such a Reynolds number in this paper.

branches of the neutral stability curves for those profiles with regions of reversed flow near the walls, the eigensolution of the Orr–Sommerfeld equation remains viscous as $R$ tends to infinity, in the sense that $kR$ tends to a finite limit. Moreover, on these lower branches the wave speed becomes negative, and substantially less than the minimum value of the basic velocity. These surprising results are further discussed in §5. In §6 a comparison of the stability calculations is made with some experimental results of Patterson (1934, 1935) and the conclusion reached that most of the available evidence is consistent with the present calculations, but that more experiments are needed to make a proper comparison.

## 2. The problem for computation

We may describe a wedge-shaped channel of divergence angle $2\alpha$ by means of co-ordinates $\xi, \eta$ defined as follows. Let $x, y$ be Cartesian co-ordinates in the physical plane, and let $z = x + iy$ and $\zeta = \xi + i\eta$. To define the co-ordinates we set $z = (b/\alpha)\, e^{\alpha\zeta}$, where $b$ is a real constant with the dimension of length. Note that $\eta = \theta/\alpha$, where $\theta$ is the usual polar angle, and that the walls of the channel are given by $\eta = \pm 1$. The curve $\xi = \text{const.}$ is a circle $|z| = (b/\alpha)\, e^{\alpha\xi}$, and $2b$ is the length of an (arbitrarily chosen) circular arc $\xi = 0$, $-1 \leqslant \eta \leqslant 1$ (figure 1). The end-points of this arc will be regarded as fixed under the limit (to be introduced presently) $R \to \infty$, $\alpha \to 0$ such that $0 \leqslant R\alpha = \gamma < 5{\cdot}46$. These co-ordinates are a special case of the more general co-ordinates $\xi, \eta$ used by Fraenkel (1963).

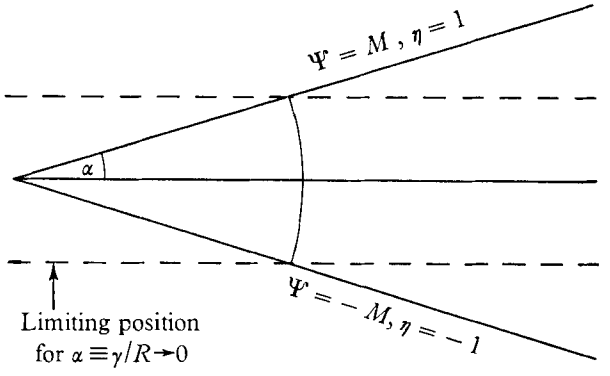


FIGURE 1. Illustration of co-ordinates for a wedge-shaped channel.

Following Fraenkel's notation we denote the stream function for a general flow by $\Psi(\xi, \eta, t)$ where $t$ is time. The volumetric flow rate is $2M$, and the kinematic viscosity is $\nu$. It is straightforward to obtain the vorticity equation in the form

$$\left[\frac{\nu}{h^2} D^2 - \frac{\partial}{\partial t} - \frac{1}{h^2}\left(\frac{\partial \Psi}{\partial \eta}\frac{\partial}{\partial \xi} - \frac{\partial \Psi}{\partial \xi}\frac{\partial}{\partial \eta}\right)\right][e^{-2\alpha\xi} D^2 \Psi] = 0, \tag{1}$$

where $D^2 \equiv \partial^2/\partial\xi^2 + \partial^2/\partial\eta^2$ and $h \equiv |dz/d\zeta| = be^{\alpha\xi}$. Upon putting $\Psi = M\psi$ and $t = (b^2/M)\,\tau$, we obtain,

$$\left[D^2 - Re^{2\alpha\xi}\frac{\partial}{\partial \tau} - R\left(\frac{\partial \psi}{\partial \eta}\frac{\partial}{\partial \xi} - \frac{\partial \psi}{\partial \xi}\frac{\partial}{\partial \eta}\right)\right][e^{-2\alpha\xi} D^2 \psi] = 0, \tag{2}$$

where $R = M/\nu$ is the Reynolds number.

The J.–H. solutions mentioned in the introduction are the steady, $\xi$-independent solution of (2), and in Fraenkel's notation are denoted by $G(\eta; R, \alpha)$. In the remainder of this paper we shall work mainly with the parameters $R$ and $\gamma$ where $\gamma = R\alpha$, and consequently we write $F(\eta; R, \gamma)$ for $G(\eta; R, \alpha)$. We denote $dF/d\eta$ by $f$. It can easily be shown from (2) that $f$ satisfies the equation

$$f''' + 4(\gamma^2/R^2)f' + 2\gamma ff' = 0, \tag{3}$$

in which a dash denotes differentiation with respect to $\eta$. Then, with the notation that $f(\eta; R, \gamma) \to w(\eta; \gamma)$ as $R \to \infty$, it can be seen from (3) that

$$f(\eta; R, \gamma) = w(\eta; \gamma) + O(\gamma^2/R^2), \tag{4}$$

and in fact Fraenkel has shown that the agreement is close. For example, with $\gamma = 4{\cdot}71$ and $R = 30$ one can deduce from table 1 of Fraenkel's (1963) paper that $w$ differs from $f$ by less than 1 %. The parameter $\gamma$ is restricted to a certain range $-\infty < \gamma < \gamma_3$ in Fraenkel's theory, where $\gamma > 0$ corresponds to outflow and $\gamma < 0$ to inflow; the value of $\gamma_3$ depends on $R$. For example, with $R = 10$, $\gamma_3 = 5{\cdot}05$; with $R = 20$, $\gamma_3 \doteqdot 5{\cdot}4$; with $R = \infty$, $\gamma_3 = 5{\cdot}46$. Within the range $-\infty < \gamma < 5{\cdot}46$, $w(\eta; \gamma)$ is an analytic function of $\gamma$, but at $\gamma = 5{\cdot}46$, $\partial w/\partial\gamma$ becomes infinite, although $w$ itself remains finite. The functions $w(\eta; \gamma)$ represent a convenient family of velocity profiles for the stability calculations; only the outflow solutions ($0 \leqslant \gamma < 5{\cdot}46$) will be considered here because their stability characteristics are certain to be more interesting than those of the inflow solutions.

In the usual way we superimpose a small disturbance $\psi_1$ and thus set

$$\psi = F(\eta; R, \gamma) + \psi_1(\xi, \eta, \tau; R, \gamma); \tag{4a}$$

and upon substituting in (2) and neglecting terms of the second degree in $\psi_1$, we obtain

$$\frac{1}{R}\left[\left(\frac{\partial}{\partial\xi} - \frac{2\gamma}{R}\right)^2 + \frac{\partial^2}{\partial\eta^2}\right] D^2\psi_1 = \left[\exp\left(\frac{2\gamma\xi}{R}\right)\frac{\partial}{\partial\tau} + f\left(\frac{\partial}{\partial\xi} - \frac{2\gamma}{R}\right)\right] D^2\psi_1 - \frac{d^2f}{d\eta^2}\frac{\partial\psi_1}{\partial\xi} - \frac{2\gamma}{R}\frac{df}{d\eta}\frac{\partial\psi_1}{\partial\eta}. \tag{5}$$

We approximate to this (virtually intractable) equation on the basis of the limit $\gamma/R \to 0$, which is presumably legitimate, at least for $|\xi| < \infty$, if either $R \to \infty$ with $\gamma$ fixed ($0 \leqslant \gamma < 5{\cdot}46$), or if $\gamma \to 0$ with $R$ fixed. If $\gamma/R$ is not small (its largest value in the present calculations is about 0·4) then this approximation amounts to the assumption of 'nearly parallel flow' made in most stability calculations; it is likely to be neither better nor worse in the present context than in stability calculations for jets (see, for example, Howard 1959, who discusses this point in more detail). Under the limit $\gamma/R \to 0$, (5) becomes

$$\frac{1}{R}D^4\psi_1 = \left(\frac{\partial}{\partial\tau} + w\frac{\partial}{\partial\xi}\right) D^2\psi_1 - \frac{d^2w}{d\eta^2}\frac{\partial\psi_1}{\partial\xi}; \tag{6}$$

and with the usual substitution

$$\psi_1(\xi, \eta, \tau) = \phi(\eta)\, e^{ik(\xi - c\tau)} \quad (k \text{ real and } \geqslant 0), \tag{7}$$

(6) reduces to the Orr–Sommerfeld equation

$$\phi^{iv} - 2k^2\phi'' + k^4\phi = ikR[\{w(\eta;\gamma) - c\}\{\phi'' - k^2\phi\} - w''(\eta;\gamma)\phi]. \tag{8}$$

Following Lin (1945, 1955) and Thomas (1953), we assume that the most unstable eigenvalue $c$ is associated with an eigenfunction $\phi$ which is even in $\eta$. The boundary conditions are then

$$\phi(-1) = \phi'(-1) = \phi'(0) = \phi'''(0) = 0. \tag{9}$$

The main computational problem tackled was to find (complex) eigenvalues $c$ for the Orr–Sommerfeld equation (8) under boundary conditions (9), when $R$, $k$ and $\gamma$ (all real) were specified.

Consider now the case of a channel with curved walls. If the curvature is sufficiently small, and with $R > 15$ (say), Fraenkel's theory and calculations show that the profiles $w(\eta;\gamma)$ are good approximations to the actual profiles. Hence if we think of $R$ as given, as $\gamma$ increases from zero the profiles given by $w(\eta;\gamma)$ approximate to those at successive stations of a channel whose divergence angle is slowly increasing.

A general description of the profiles $w(\eta;\gamma)$ is as follows. For $\gamma = 0$, there results $w(\eta;0) = (\frac{3}{2})(1-\eta^2)$, i.e. the usual Poiseuille flow. As $\gamma$ increases, the curvature of the profile changes, until at $\gamma = 1{\cdot}80$ points of inflexion occur at the walls. As $\gamma$ continues to increase, the points of inflexion move inwards towards the centre of the channel. For $\gamma = 4{\cdot}71$ we have the separation profile for which $w' = 0$ at the walls. For $4{\cdot}71 < \gamma < 5{\cdot}46$, there are regions of reversed flow at each side of the channel. The flow cannot be analytically continued by any symmetric J.–H. function beyond $\gamma = 5{\cdot}46$ owing to the singularity in $w$ as a function of $\gamma$. It should be mentioned here that profiles with regions of reversed flow are not of purely academic interest for they have been actually observed (see Patterson 1934).

Different formulae are required for $w$ in different ranges of $\gamma$. These formulae are given by Fraenkel (1963, 1962) and some details are given in the Appendix. The two different formulae given are for the same analytic function of $\gamma$. It will be noted that these formulae do not give $w(\eta;\gamma)$ explicitly in terms of $\gamma$, and in our calculations $\gamma$ actually appeared as a result of the choice of another parameter. This accounts for the strange values of $\gamma$ which will appear later, in the results.

Typical profiles are shown in association with their neutral curves in figures 2, 3, 4 and 5, points of inflexion being marked by the letter $S$.

## 3. Computation of the Orr–Sommerfeld problem

### 3.1 *Method*

Let us first recall that the problem selected for computation was the Orr–Sommerfeld equation (8) together with the boundary conditions (9) for even $\phi$. If $R$, $k$ and $\gamma$ (all real) are specified this is an eigenvalue problem for $c$, which will be complex in general. Writing $c = c_r + ic_i$, we note that a disturbance of the form (4$a$) is amplified or damped with time according to whether $c_i$ is positive or negative. If any eigenvalues exist with positive $c_i$ then the flow is regarded as unstable to infinitesimal disturbances.

In our approximation the parameter $\gamma$ specifies the basic flow, and the primary aim is to find $R_{\text{crit}}$ as a function of $\gamma$, $R_{\text{crit}}$ being the lowest value of $R$ for which an unstable ($c_i > 0$) mode exists. If we fix $\gamma$, there is in each $(R, k)$-plane a neutral curve on which the imaginary part of the most unstable $c$ is zero. It is possible to find $R_{\text{crit}}$ by first finding these neutral curves. We are also interested in the behaviour of the eigenfunctions and eigenvalues as $R \to \infty$ on both the upper and lower branches of the neutral curves.

The eigenvalue problem was reduced to a matrix eigenvalue problem by the finite difference technique used by Thomas (1953) and by Kurtz & Crandall (1962). By means of the transformation

$$g = \phi - \tfrac{1}{6}h^2\phi'' + \tfrac{1}{60}h^4\phi^{\text{iv}},$$

where $h$ is the step length in $\eta$, the truncation error in the representation of the derivatives of $\phi$ by up to fourth central differences of $g$ is reduced to $O(h^6)$ for $\phi''$ and $O(h^4)$ for $\phi^{\text{iv}}$, that is to one order in $h^2$ better than by using merely fourth differences of $\phi$.

The eigenvalue problem is then reduced to solving an equation of the form $\det[A(k, R, \gamma; c)] = 0$ where $[A]$ is a matrix of complex elements, of the five-band type except for some extra elements for the boundary conditions, and $c$ is the required eigenvalue. A programme to evaluate this determinant efficiently was written; also a root-finding routine which, given three values of $c$ near to a root, iterates (by means of a complex quadratic curve) to find the root to a selected degree of accuracy.

Starting from a value of $c$ given by Thomas for $\gamma = 0$ (Poiseuille flow), $R = 1667$ and $k = 1$ (Thomas's $R$ being 2500) it was possible to find $c$ for all relevant values of the parameters $\gamma$, $k$ and $R$ by changing them in small steps. Hence the neutral curves in the $(R, k)$-planes (for fixed $\gamma$) could be drawn by interpolating to values of $R$ and $k$ for which $c_i = 0$. In fact, an automatic procedure for tracing the neutral curves was programmed, requiring merely two points near the upper branch to start.

Contour plots of the modulus of the determinant may be made in the complex $c$-plane (for fixed values of $\gamma$, $R$ and $k$) in order to locate zeroes. To confirm that the value of $c$ being traced was that of greatest imaginary part, extensive plots were made for a Poiseuille-flow case and for the case $\gamma = 3{\cdot}07$, $R = 1667$ and $k = 1$. No evidence was found of any roots with greater $c_i$, though there were many with smaller $c_i$. There is also a check on this point for small $kR$ by a method given in §5.

### 3.2. *Accuracy and checks*

If $w(\eta; \gamma)$ is replaced by a constant $w_0$, it can be shown that the eigenvalues are given by $c = w_0 - i(s^2 + k^2)/kR$, where $s$ is a root of the equation $s \tan s = -k \tanh k$. This was used as a first check.

For $\gamma = 0$ (Poiseuille flow), Thomas (1953) gives values of $c$, for various $R$ and $k$, to 4 decimal places. These results were reproduced by the present programme for the cases $R < 2000$ using 40 steps. For larger $R$, Thomas's results were consistent with ours for 20 and 40 steps on the assumption of an error proportional to $h^4$. With 40 steps it is estimated that, for the cases computed, our

programme obtained $c$ correct to 4 decimal places when $kR < 2000$, and, taking into account the rate of variation of $c_i$ with $k$ and with $R$, the possible error in $k$ for a given $R$ on the calculated curves was estimated to be less than 0·002 in general. The critical values of $R$ were estimated to have an error of less than 0·5 %.

Other checks will appear in the course of the presentation and development of the results.

## 4. Main results

### 4.1. *The critical Reynolds number*

The neutral curves for $\gamma = 1{\cdot}09$, 3·07, 4·71 and 5·45 are shown in figures 2–5, together with the corresponding velocity profiles. Limiting values of $k, c$ and $kR$ as $R \to \infty$ (on these curves) are marked, and these are explained in §4.2.

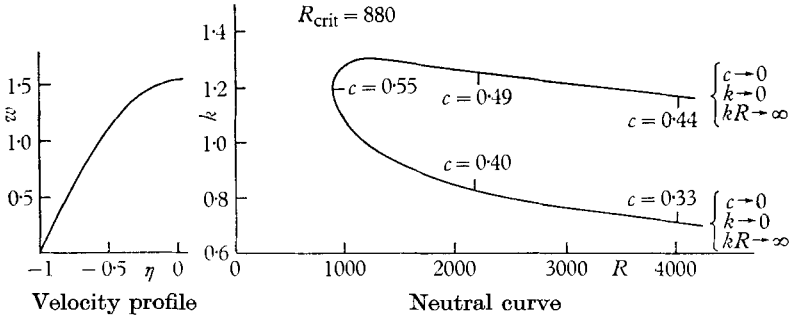


FIGURE 2. Velocity profile and neutral curve for $\gamma = 1{\cdot}09$.

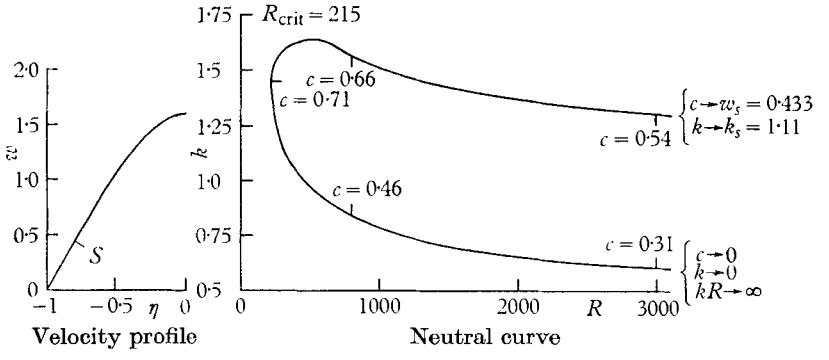


FIGURE 3. Velocity profile and neutral curve for $\gamma = 2{\cdot}06$.

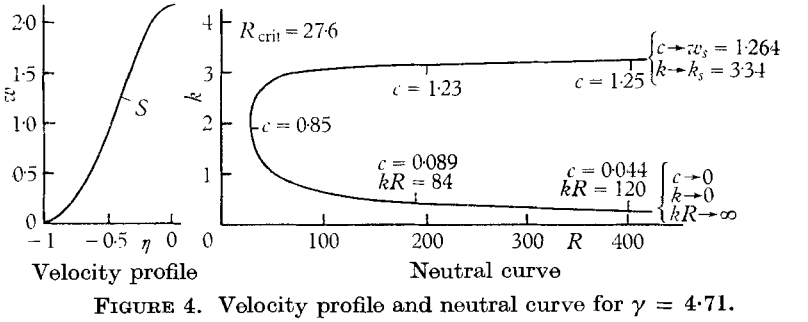


FIGURE 4. Velocity profile and neutral curve for $\gamma = 4{\cdot}71$.

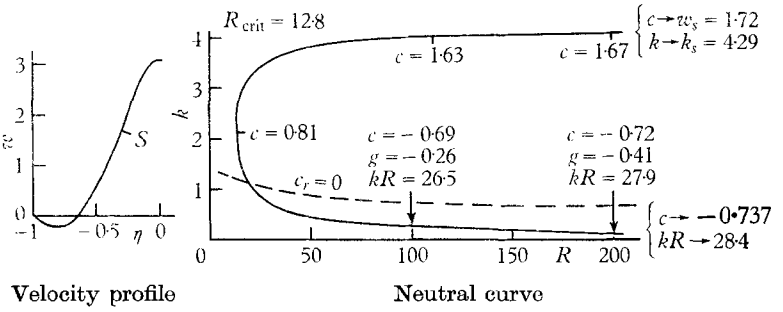


FIGURE 5. Velocity profile and neutral curve for $\gamma = 5{\cdot}45$. Here, on the neutral curve, $c$ is the wave velocity and $g$ is the group velocity.

It will be noticed that the value of $R_{crit}$ descends drastically as $\gamma$ increases. The neutral curves shown are a selection of ten actually computed and a graph of $R_{crit}$ vs $\gamma$ is shown in figure 6 for $\gamma$ between 2 and 5·45. This diagram is translated into the $(R, \alpha)$-plane in figure 7. Some experimental results are also marked in figures 6 and 7, and these are discussed in § 6.

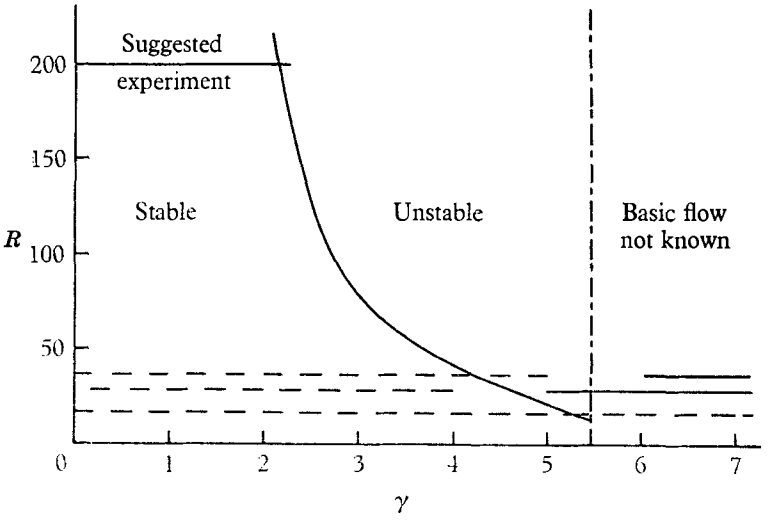


FIGURE 6. $R_{crit}$ versus $\gamma$ ($\equiv R\alpha$), with some results of Patterson's experiments. Observed by Patterson: – – – – symmetric flows; —— unsymmetric flows.

For $\gamma = 0$ (Poiseuille flow), we know from the calculations of Thomas (1953) that $R_{crit}$ ($R \equiv M/\nu$ here) is about 3910 for $\gamma = 0$; it decreases to 12·8 for $\gamma = 5{\cdot}45$. At this stage it is of the same order of magnitude as $R_{crit}$ for two-dimensional jets (see, for example, Howard 1959). There is here a very striking decrease; for example, if we had a portion of channel with the semi-angle $\alpha$ equal to 0·01 radians, the flow would become unstable at about $R = 215$, compared with $R = 3910$ for a parallel-walled channel.

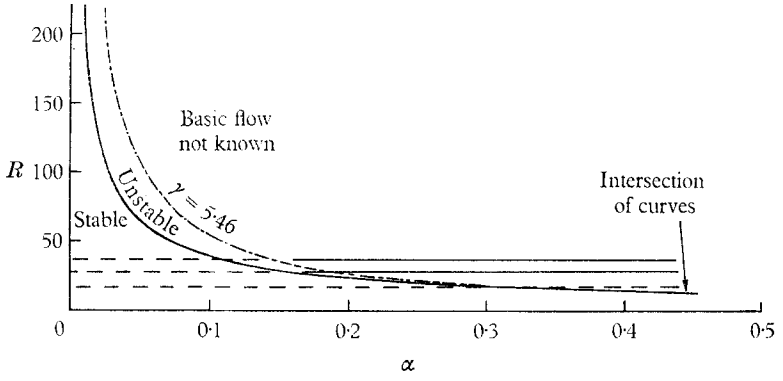


FIGURE 7. $R_{crit}$ versus $\alpha$, with some results of Patterson's experiments. Observed by Patterson: – – – – symmetric flows; —— unsymmetric flows.

### 4.2. *The neutral curves for large Reynolds number*

(i) On the neutral curves (figures 2–5) there are shown values of $c$ and $kR$ at selected points, and limiting values of $c, k$ and $kR$ as $R \to \infty$. The limiting values could not, of course, be obtained directly from the neutral-curve calculations: where $kR \to \infty$ they are related to solutions of the inviscid Rayleigh problem

$$\left.\begin{aligned} \phi'' - k^2\phi - \frac{w''}{w-c}\phi = 0, \\ \phi(-1) = 0, \quad \phi'(0) = 0. \end{aligned}\right\} \tag{11}$$

(ii) The most interesting and unexpected of the limits shown on the neutral curves is that for the lower branch in figure 5, for $\gamma = 5{\cdot}45$. This is typical of the lower branches when $\gamma > 4{\cdot}71$, that is when the velocity profile has reversed flow near the walls. The eigensolution remains viscous as $R \to \infty$ along the lower branch (that is, $kR$ tends to a finite limit), and the wave speed $c_r$ tends to a negative value which is substantially less than the minimum value of the basic velocity. The curve $c_r = 0$ in the $(R, k)$-plane for $\gamma = 5{\cdot}45$ is shown in figure 5, and it is seen that amplified ($c_i > 0$) waves with negative wave velocity ($c_r < 0$) occur only when $R > 15$, as compared with $R_{crit} = 12{\cdot}8$. One would not necessarily expect a physical realization of these 'backward' waves since, according to our calculations the flow would have already become unstable when they are possible. In any case, in thinking of the propagation of an actual physical disturbance, presumably the group velocity $g = d(kc_r)/dk$ is the more appropriate measure of its speed of movement. This has been calculated on the neutral curve for $\gamma = 5{\cdot}45$: for $R = 50$, $g = 0{\cdot}09$; for $R = 100$, $g = -0{\cdot}26$; for $R = 200$, $g = -0{\cdot}41$. Thus, on the basis of a group velocity, actual physical disturbances moving upstream seem even more unlikely.

In view of the finite limiting value of $kR$, the theorem for the Rayleigh problem that $w_{min} \leqslant c \leqslant w_{max}$ need not hold in the limit as $R \to \infty$; nevertheless the fact that the wave velocity lies outside the velocity range of the basic flow seems surprising at first sight and so these results were later made more precise and confirmed by a method described in § 5.

(iii) In connexion with the limits on the lower branches, it should be remembered that Lin in his fundamental papers (1945) and again in his book (1955) gives an asymptotic analysis of the neutral curves for general symmetric velocity profiles in a channel with (in our notation) $w' > 0$ in $-1 \leqslant \eta < 0$. It follows from Lin's work that along the lower branch as $R \to \infty$ the eigensolution tends to

$$\phi \propto w, \quad c = 0, \quad k = 0, \tag{12}$$

which is the well-known 'trivial' solution of the Rayleigh problem; and these limits are marked on the lower branches in figures 2 and 3, for which the corresponding profiles fulfil the conditions assumed by Lin. The limits $c \to 0$, $kR \to \infty$ on the lower branch of figure 5, which is the neutral curve for the separation profile, are the only ones possible if these limits are to vary in a continuous manner with $\gamma$. However, when $w'(-1) \leqslant 0$, Lin's method is clearly not applicable as it stands (see, for example, Lin (1955), equation 3·6·12), and we might therefore expect some sort of transition in the asymptotic behaviour of the neutral curve when $w'(-1)$ becomes negative. Also, on general grounds, we would no longer expect the eigenfunction $\phi$ to tend to $w$ as $R \to \infty$ when regions of reversed flow exist, for this would be a more oscillatory eigenfunction which would not be expected to be associated with the most unstable eigenvalue.

(iv) For the limits on the upper branches when $\gamma < 1{\cdot}80$, that is when no point of inflexion occurs in the basic velocity profile, it follows from Lin's analysis that the eigensolution tends to (12) as $R \to \infty$; and the computed values showed a steady decrease in $c$ and in $k$ as $R$ was increased, although they could not be calculated very close to the limit because the programme becomes increasingly inaccurate as $kR$ is increased.

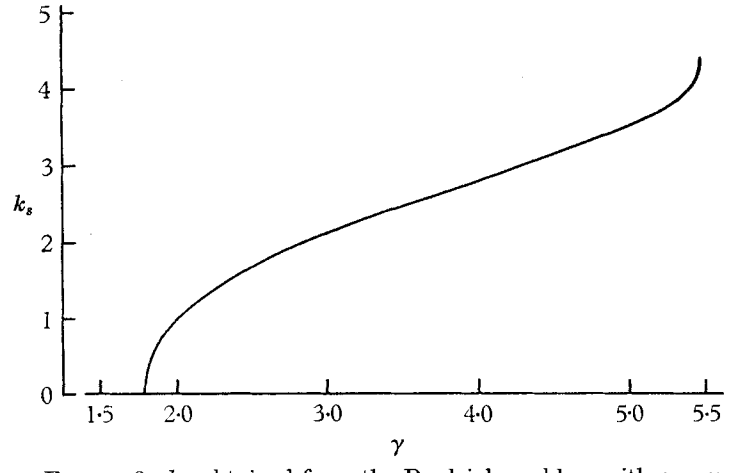


FIGURE 8. $k_s$, obtained from the Rayleigh problem with $c = w_s$.

(v) We now consider the upper branches when $\gamma > 1{\cdot}80$, that is when there is a point of inflexion $S(\eta = \eta_s, w = w(\eta_s, \gamma) = w_s)$ in the velocity profile. As is well known (see Lin 1955, §8.2), if we substitute $c = w_s$ in the Rayleigh problem (11) and regard the wave-number $k = k_s$ as the desired eigenvalue, then a real

positive $k_s$ does in fact exist. It is then to be expected that, as $R \to \infty$ along the upper branch of the neutral curve, we shall have $k \to k_s$ and $c \to w_s$. Lin (1945, Part III) has also shown that such behaviour is to be expected, from his asymptotic analysis of the neutral curve, although his proof holds only for small $w_s$ and $w'(-1) > 0$.

The solution of the Rayleigh problem was computed as follows. For prescribed $\gamma$ and with $c = w_s$ a series of values of $k$ near $k_s$ was estimated from the numerical results for the Orr–Sommerfeld problem. The Rayleigh equation, with initial conditions $\phi(-1) = 0$, $\phi'(-1) = 1$ was then integrated from $\eta = -1$ to $\eta = 0$ by a Runge–Kutta process; and $k_s$ was found by interpolation, from the requirement that $\phi'(0) = 0$. The values of $k_s$ and $w_s$ were found to agree well with the values of $k$ and $c$ for large but finite $R$ from the neutral-curve calculations in the whole range $1{\cdot}80 < \gamma < 5{\cdot}46$. For example, with $\gamma = 3{\cdot}07$, $w_s = 0{\cdot}901$, and with $c = w_s$ the Rayleigh problem gave $k_s = 2{\cdot}16$, while the neutral curve calculation gave $c = 0{\cdot}903$, $k = 2{\cdot}164$ at $R = 3200$. A graph of $k_s$ vs $\gamma$ is shown in figure 8.

## 5. Further discussion of the lower branch

### 5.1. *Limiting values of kR and c*

If $k = O(R^{-1})$ as $R \to \infty$, the limiting differential equation is no longer the Rayleigh equation but

$$\phi^{\mathrm{iv}} = i\lambda\{(w-c)\phi'' - w''\phi\}, \quad \text{where} \quad \lambda = \lim_{R\to\infty} kR. \tag{13}$$

With boundary conditions (9), equation (13) may be regarded, if $\lambda$ and $\gamma$ are given, as an eigenvalue problem in $c$. The relevant question is: for a given $\gamma$, which real values of $\lambda$ (if any) will produce an eigenvalue $c$ with $c_i = 0$, and what

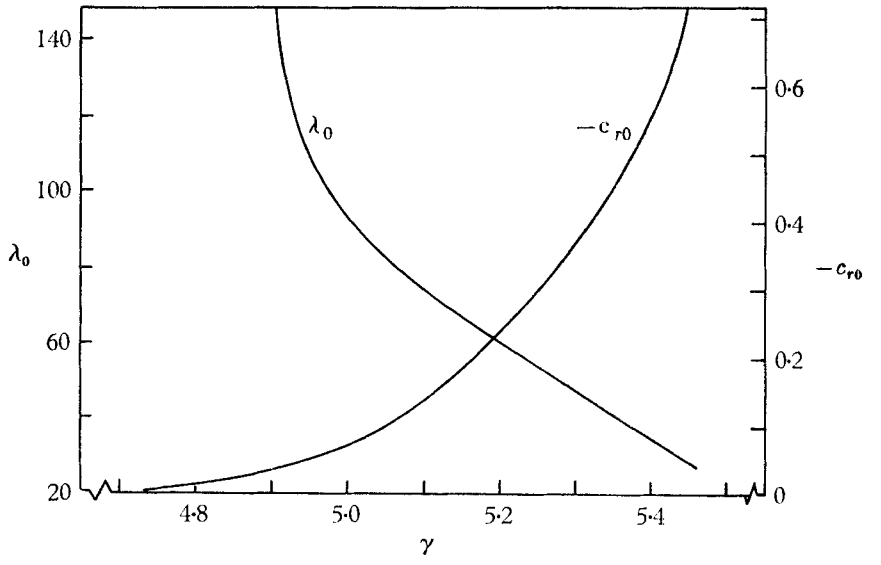


FIGURE 9. Limiting values of $kR$ and of $c$ as $R \to \infty$ on the lower branch, denoted by $\lambda_0$ and $c_{r0}$.

then is the value of $c_r$? A modification of the programme for the Orr–Sommerfeld problem was used to solve this problem. In figure 9 the resulting values, $\lambda_0$ and $c_{r0}$, are plotted against $\gamma$. These were found to agree well with the neutral-curve calculations for the lower branch and large but finite $R$. For example, for the case with $\gamma = 5{\cdot}45$: for $R = 503{\cdot}9$ and $k = 0{\cdot}0562$, $Rk = 28{\cdot}3$ and $c = -0{\cdot}7347 + 0{\cdot}0000i$; for $R = 1103$ and $k = 0{\cdot}0257$, $Rk = 28{\cdot}4$ and $c = -0{\cdot}7365 + 0{\cdot}0000i$; while the limiting values calculated from equation (13) were found to be $\lambda_0 = 28{\cdot}41$ and $c_{r0} = -0{\cdot}7369$.

### 5.2. *Eigensolutions for small kR*

In relation to the negative values of $c_r$ obtained on the lower branches, it is of interest to study the solutions of the Orr–Sommerfeld equation (8) for small $k$. We shall not at first restrict this study to even eigenfunctions, but will use the more general boundary conditions

$$\phi(-1) = \phi'(-1) = \phi(1) = \phi'(1) = 0. \tag{14}$$

It will be shown below that for a given velocity profile $w$ there appears to be a set of eigensolutions with the property that $c_i \sim O(k^{-1})$ as $k \to 0$ with $R$ fixed. The existence of negative $c_r$ for the least stable of these eigensolutions is shown for small $kR$, for certain types of velocity profile.

The method is prompted by the observation that if in (8) we let $k \to 0$ with $R$ and $c$ bounded the differential equation reduces to $\phi^{\mathrm{iv}} = 0$, which has no eigensolutions. The most probable way out of this anomaly is that $c \sim O(k^{-1})$ for $k \to 0$. We are thus led to try the expansions

$$c^{(n)} = c_0^{(n)}/k + c_1^{(n)} + c_2^{(n)}k + \ldots, \tag{15}$$

$$\phi^{(n)}(\eta) = \phi_0^{(n)}(\eta) + k\phi_1^{(n)}(\eta) + k^2\phi_2^{(n)}(\eta) + \ldots, \tag{16}$$

where $n$ is the label of the $n$th eigensolution of (8) with boundary conditions (14).

Substituting in (8) and equating powers of $k$, we obtain

$$\phi_0^{(n)\mathrm{iv}} + iRc_0^{(n)}\phi_0^{(n)\prime\prime} = 0, \tag{17}$$

$$\phi_1^{(n)\mathrm{iv}} + iRc_0^{(n)}\phi_1^{(n)\prime\prime} = iR(w\phi_0^{(n)\prime\prime} - c_1^{(n)}\phi_0^{(n)\prime\prime} - w''\phi_0^{(n)}) \tag{18}$$

and in general

$$\phi_m^{(n)\mathrm{iv}} + iRc_0^{(n)}\phi_m^{(n)\prime\prime} = F_m(R;\, c_0^{(n)}, \ldots, c_m^{(n)};\, \phi_0^{(n)}, \ldots, \phi_{m-1}^{(n)};\, w), \tag{19}$$

where the explicit form for the function $F_m$ can easily be found but is not required here.

We first note the eigensolutions of (17) with boundary conditions (14), which may be expected to approximate to the eigensolutions of (8) for small $k$. For even eigenfunctions they are given by

$$\phi_0^{(2p)} = \cos\lambda_{2p}\eta - \cos\lambda_{2p}, \tag{20}$$

where $\lambda_{2p} = (p+1)\pi$ for $p = 0, 1, 2, \ldots.$

For odd eigenfunctions they are given by

$$\phi^{(2p+1)} = \eta \sin \lambda_{2p+1} - \sin \lambda_{2p+1} \eta, \tag{21}$$

where the $\lambda_{2p+1} (p = 0, 1, 2, \ldots)$ are the positive roots of the equation $\tan \lambda = \lambda$. In each case the appropriate eigenvalue is

$$c_0^{(n)} = -\frac{i\lambda_n^2}{R}. \tag{22}$$

It can easily be seen that the least stable of the eigenvalues (22) is $c_0^{(0)} = -i\pi^2/R$, and this is associated with the *even* eigenfunction

$$\phi_0^{(0)} = \cos \pi\eta + 1 \tag{23}$$

in accord with the assumption made in § 2.

Since $iRc_0^{(n)}$ is real, the operator consisting of the differential operator

$$\frac{d^4}{dy^4} + iRc_0^{(n)} \frac{d^2}{dy^2}$$

and the boundary conditions (14) may be shown to be self-adjoint. For a self-adjoint operator $\mathscr{L}$ we have the general result that $\mathscr{L}\phi_m = F_m$ has a solution if and only if $F_m$ is orthogonal to every solution $Z$ of $\mathscr{L}Z = 0$. In our case, with $c_0^{(n)}$ specified, there is only one solution $\phi_0^{(n)}$ to the equation $\mathscr{L}Z = 0$, and so

$$\int_{-1}^{1} F_m \phi_0^{(n)} \, d\eta = 0 \tag{24}$$

is the corresponding condition for $\phi_m^{(n)}$ to be a solution of (19). Alternatively, the necessity for the condition (24) is easily shown by multiplying (19) by $\phi_0^{(n)}$ and (17) by $\phi_m^{(n)}$, integrating from $\eta = -1$ to $\eta = 1$, and subtracting.

Since we are interested in the least stable eigensolution, we apply condition (24) with $n = 0$ and for $m = 1$ this yields, after some partial integration,

$$c_1^{(0)} = \int_{-1}^{0} w\{\phi_0^{(0)} \phi_0^{(0)\prime\prime} + 2(\phi_0^{(0)\prime})^2\} d\eta \Big/ \int_{-1}^{0} (\phi_0^{(0)\prime})^2 \, d\eta. \tag{25}$$

The function $\phi_1^{(0)}$ may now be found by the method of 'variation of parameters' from equation (18), and the process extended. But the series for $c$ proceeds in powers of $k$ and of $kR$ and on the neutral curve $kR$ is too large for only a few terms to be useful. Nevertheless, some information may be obtained from just the first two terms of the series (15). If $c$ is the least stable eigenvalue we have, for small $kR$,

$$c_i = c_0^{(0)}/k + O(kR) = -\pi^2/kR + O(kR),$$
$$c_r = c_1^{(0)} + O(k^2R^2).$$

It should be noted that $c_1^{(0)}$ is independent of $R$, so that for a given profile $c_r$ tends to the same value as $k \to 0$ for all values of $R$. The above values were found to agree closely with eigenvalues calculated from the main eigenvalue programme described in § 2. For example, with $\gamma = 5{\cdot}45$, $R = 200$ and $k = 0{\cdot}001$ the main programme gave $c = -1{\cdot}3033 - 49{\cdot}335i$, and a calculation of $c_1^{(0)}$ from (25) by numerical quadrature gave $c_1^{(0)} = -1{\cdot}3034$ while $(\pi^2/kR) = 49{\cdot}348$ in this case.

It was observed (from figures from the main programme) that $c_r$ always increases with $k$ for any fixed $R$, and so it appears that the quantity $c_1^{(0)}$ is the minimum value for $c_r$, and is related to the appearance of the negative values of $c$ on the neutral curves. It is fairly easy to see from (25) that $c_1^{(0)}$ is more likely to

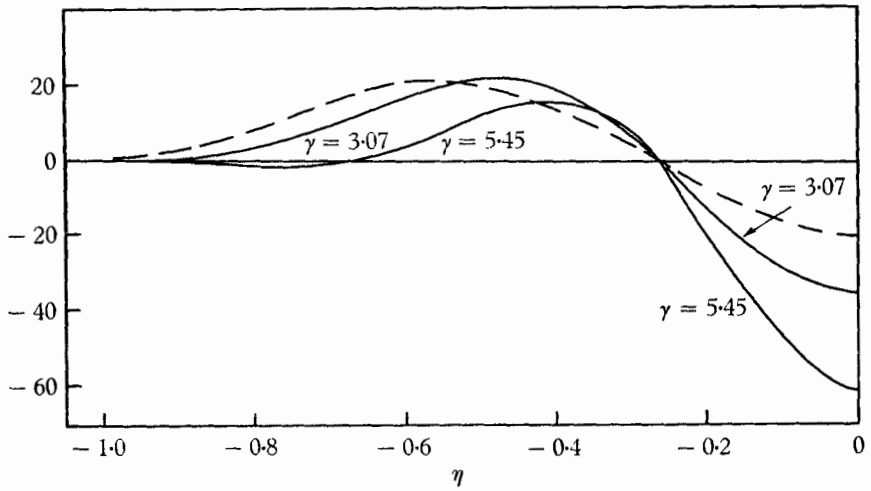


FIGURE 10. The broken curve shows the function $\phi_0^{(0)}\phi_0^{(0)\prime\prime} + 2(\phi_0^{(0)\prime})^2$. The continuous lines show the function $w\{\phi_0^{(0)}\phi_0^{(0)\prime\prime} + 2(\phi_0^{(0)\prime})^2\}$ for $\gamma = 5{\cdot}45$ and $\gamma = 3{\cdot}07$, showing how the integral of this function changes sign.

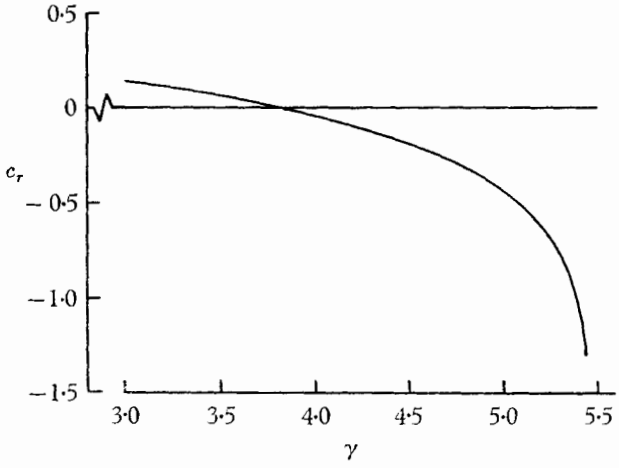


FIGURE 11. Values of $c_r$ at $k = 0$.

be negative when the velocity profile $w$ has regions of reversed flow. Graphs of $\phi_0^{(0)}\phi_0^{(0)\prime\prime} + 2(\phi_0^{(0)\prime})^2$ and of this function multiplied by $w$ are shown in figure 10, and values of $c_r$ at $k = 0$ calculated from (25) are shown in figure 11 plotted against $\gamma$. This goes some way towards explaining the negative $c$ values; but shows nothing of the critical role of the sign of $w'(-1)$ indicated in § 4.2.

### 5.3. *Some limiting eigenfunctions*

Some limiting eigenfunctions as $R \to \infty$ on the lower branches were computed by integrating equation (13) once to give

$$\phi''' = i\lambda\{(w-c)\,\phi' - w'\phi\} + \text{const.}, \tag{26}$$

and since $\phi'(0) = \phi'''(0) = 0$ and also $w'(0) = 0$, the constant is zero. Hence, if we specify $\gamma$ and insert the appropriate values $\lambda_0$ and $c_{r0}$ for $\lambda$ and $c$, and starting with $\phi = \phi' = 0$ at $\eta = -1$ integrate equation (26) by a step-by-step process up to $\eta = 0$, we generate the eigenfunction. This also gives another check on the values of $\lambda_0$ and $c_{r0}$, for we should find $\phi' = 0$ at $\eta = 0$.

This was done by a Runge–Kutta process, and the values of $\lambda_0$ and $c_{r0}$ shown in figure 9 were confirmed. Graphs of the real and imaginary parts, $\phi_r$ and $\phi_i$, of $\phi$ are shown in figure 12 for $\gamma = 5{\cdot}38$ and $\gamma = 4{\cdot}92$. These were calculated with $\phi''(-1) = 1$, a purely arbitrary condition chosen for convenience. It appears that as $\gamma$ approaches 4·71 from above the eigenfunctions approach $w(\eta;\ 4{\cdot}71)$ as expected. Actually, the real part of the eigenfunction differs very little from a multiple of $w(\eta;\ 4{\cdot}71)$ for all calculated cases in the range $4{\cdot}71 < \gamma < 5{\cdot}46$, although the imaginary part changes more rapidly with $\gamma$.

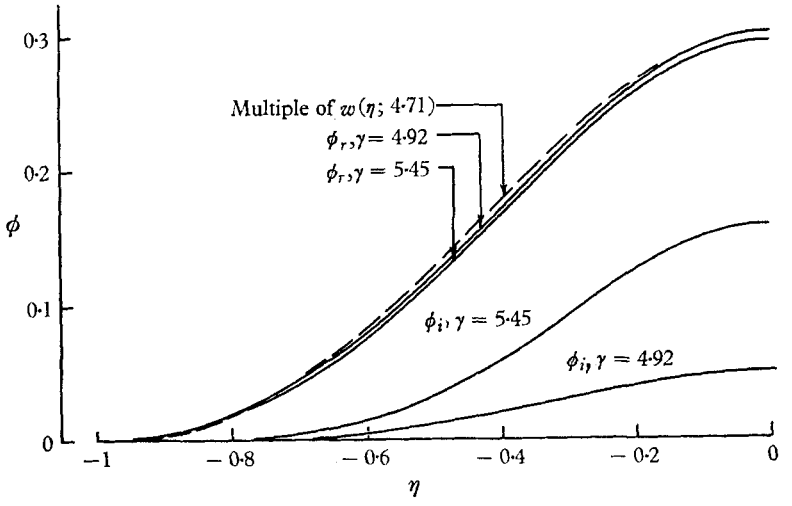


FIGURE 12. Limiting eigenfunctions as $R \to \infty$ along the lower branches. These eigenfunctions were calculated with the (arbitrary) condition $\phi''(-1) = 1 + i0$. The broken line shows $w(\eta;\ 4{\cdot}71)$ scaled to be equal to $\phi_r$ for $\gamma = 4{\cdot}92$ at $\eta = 0$.

## 6. Experimental evidence

Patterson (1934, 1935) performed experiments on two-dimensional flow in a divergent channel in which the semi-divergence angle $\alpha$ gradually increases from zero up to about 0·5 radians. Although these experiments were not performed to investigate stability, a limited amount of information may be gleaned from the results.

Fraenkel (1963) has shown that the velocity profiles observed by Patterson at $R(\equiv M/\nu) = 17{\cdot}5$ are closely approximated by the family $w(\eta;\ \gamma)$ for values of $\gamma$ up to 4·34. From the point of view of the present stability calculations, these flows fall into our calculated stable region in the $(R, \gamma)$-plane (figure 6) or equivalently in the $(R, \alpha)$-plane (figure 7), and so these observations are consistent with our calculations.

Before discussing some other results of Patterson we should recall that the solutions $w(\eta;\gamma)$ extend only as far as $\gamma = 5{\cdot}46$. At $\gamma = 5{\cdot}46$ there is a singularity in our approximate solution $w(\eta;\gamma)$ and the steady-state solution near $\gamma = 5{\cdot}46$ and for $\gamma > 5{\cdot}46$, if it exists, is not known. We expect that if a steady-state flow exists for $\gamma > 5{\cdot}46$, it may be different in nature from the symmetric type preceding it, but of this we are not certain. For $R = 28{\cdot}4$, $\gamma \doteq 4{\cdot}5$ and for $R = 37{\cdot}6$, $\gamma \doteq 5{\cdot}5$, Patterson's photographs show a departure from laminar symmetric flow to laminar unsymmetric flow, with separation of the main stream from one wall. For lower values of $\gamma$ the flow appears to be nearly symmetric although we do not know whether the profiles are close to the family $w(\eta;\gamma)$ as Patterson did not measure profiles for these Reynolds numbers. It is impossible to locate a precise value of $\gamma$ at which the flow starts to become unsymmetric. This is indicated in our figures 6 and 7.

Patterson reports that this flow pattern, of a symmetric laminar flow up to a certain point in the channel and then an unsymmetric laminar flow, remains steady, once it is established. It could be regarded, perhaps, as coming into existence for one or both of two reasons: either because the symmetric flow which is theoretically possible for $\gamma$ up to 5·46 is unstable at some lower value of $\gamma$ (note that our even $\phi(\eta)$ produces an anti-symmetric disturbance velocity parallel to the stream); or because of a basic property of the exact steady-state solution, linked with the singularity of $w(\eta;\gamma)$ at $\gamma = 5{\cdot}46$. It is obviously very difficult to distinguish between these possibilities by any experiment at a Reynolds number close to 12, which is the value at the intersection of the stability boundary and the boundary $\gamma = 5{\cdot}46$, because we would be trying to locate a transition in a rather small range of $\gamma$. For example, at $R = 20$ the flow becomes unstable at $\gamma = 5{\cdot}1$ by the calculations, but the singularity in the approximate solution is at $\gamma = 5{\cdot}46$. In any case, owing to the approximation made in the stability calculations of neglecting terms in $\gamma/R$ the calculations in this region of the $(\gamma, R)$-plane may not be meaningful. Also, the effects of wall curvature on the stability have been completely neglected. Therefore we cannot take Patterson's results to be very significant in the context of our stability problem.

Nevertheless, on the supposition that the occurrence of unsymmetric flow is linked solely with the singularity at $\gamma = 5{\cdot}46$, figure 4 of Patterson's (1934) paper would be distinctly puzzling. For $R = 17{\cdot}2$ this shows laminar symmetric flow up to $\gamma \doteq 6$ and probably up to $\gamma \doteq 8{\cdot}5$, though the detail is not clear and there could be the beginnings of fluctuating disturbances for $\gamma > 6$. There is certainly no transition to unsymmetric flow near $\gamma = 5{\cdot}46$. We must conclude that there is some basic difference in the situation here. It could be that the mechanism of transition to unsymmetric flow is in fact related to the infinitesimal instability of our calculations, and that at $R = 17{\cdot}2$ the motion is truly stable

for $\gamma$ up to about 8, although our analysis holds only up to $\gamma \doteq 5{\cdot}46$ and shows instability at $\gamma = 5{\cdot}3$. However, our various approximations are highly questionable here and it is possible that the true stability boundary calculated for the true velocity profiles should be higher at its lower end than shown in figure 6. Obviously more experiments are needed.

It would, for example, be informative to perform an experiment in a channel where $\alpha$ increased slowly to a small value $\alpha_1$, and then remained constant for a considerable length of channel. If $R$ were gradually increased we should expect a sequence of the J.–H. profiles to be exhibited in the straight-walled portion of the channel, and then we would expect instability to occur when $R$ reached a certain value. For example, with $\alpha_1 = 0{\cdot}01$ the flow becomes theoretically unstable when $R = 215$. The value of $\gamma$ would then be 2·15 in the straight-walled part, and we could distinguish between any observed instability and between the possible transition at $\gamma \doteq 5{\cdot}46$. The relation between experiment and our calculations should, of course, be better the smaller the value of $\alpha_1$, since the neglected terms are $O(\gamma/R) = O(\alpha_1)$ here. It would be interesting to see whether any regular oscillatory disturbances were set up, or whether the whole straight-walled portion became turbulent, or whether the flow changed rapidly over to an unsymmetric form at a certain value of $R$.

This work was initiated at Imperial College where the author is a part-time student. Thanks are due to Mr L. E. Fraenkel for supervising the work, to Dr J. T. Stuart for suggesting the use of equations (13) and (26), and to Dr A. W. Gillies and Professor R. S. Scorer for their interest; also to the staff of London University Computing Centre for their help.

## Appendix

*The formulae for the velocity profiles*

*J.–H. I solutions*, $0 \leqslant \gamma \leqslant 2{\cdot}82$

We may specify $m$ in the range $0{\cdot}5 \leqslant m < 1$ and find $a$ by solving

$$3\,\mathrm{sn}^2(a|m)\,\mathrm{dc}^2(a|m) = 4m - 2. \tag{A 1}$$

Then, with

$$\rho = 2E(a|m) - a - \mathrm{sn}\,(a|m)\,\mathrm{dc}\,(a|m) + a\,\mathrm{sn}^2(a|m)\,\mathrm{dc}^2(a|m), \tag{A 2}$$

we find

$$\gamma = 6a\rho, \tag{A 3}$$

and

$$w(\eta;\gamma) = \{a/\rho\}\{\mathrm{sn}^2(a|m)\,\mathrm{dc}^2(a|m) - \mathrm{sn}^2(a\eta|m)\,\mathrm{dc}^2(a\eta|m)\}. \tag{A 4}$$

*J.–H. $II_1$, and J.–H. $II_2$ solutions*, $2{\cdot}82 \leqslant \gamma < 5{\cdot}46$

We may specify $m$ which first decreases from 1 to 0·5 and then increases again to 0·57 and we then find $b$ as the solution of

$$3m\,\mathrm{cn}^2(b|m) = 2m - 1 \tag{A 5}$$

in such a way that $\mathrm{cn}\,(b|m)$ increases as $m$ varies as described above, while $0 \leqslant b \leqslant 2K$.

Then with $$\rho = E(b|m) - b\,\mathrm{dn}^2(b|m) \tag{A 6}$$

we find $$\gamma = 6bp \tag{A 7}$$

and $$w(\eta;\gamma) = \{mb/\rho\}\{\mathrm{sn}^2(b|m) - \mathrm{sn}^2(b\eta|m)\}. \tag{A 8}$$

## REFERENCES


FRAENKEL, L. E. 1962 *Proc. Roy. Soc.* A, **267**, 119.

FRAENKEL, L. E. 1963 *Proc. Roy. Soc.* A, **272**, 406.

HOWARD, L. N. 1959 *J. Math. Phys.* **37**, 283.

KURTZ, E. F. & CRANDALL, S. H. 1962 *J. Math. Phys.* **41**, 264.

LIN, C. C. 1945 *Quart. Appl. Math.* **3**, Pts. I, II, III, pp. 117, 218, 277.

LIN, C. C. 1955 *The Theory of Hydrodynamic Stability*. Cambridge University Press.

PATTERSON, G. N. 1934 *Canad. J. Res.* **11**, 770.

PATTERSON, G. N. 1935 *Canad. J. Res.* **12**, 676.

THOMAS, L. H. 1953 *Phys. Rev.* (2) **91**, 780.